Available online at www.sciencedirect.com
SCIENCE DIRECT®
Pergamon
Acta Materialia 51 (2003) 1899–1907
Acta MATERIALIA
www.actamat-journals.com

Bulk metallic glasses in the Zr-Al-Ni-Cu system

W. Chen [ab], Y. Wang [a], J. Qiang [a], C. Dong [a,*]

[a] *State Key Laboratory for Materials Modification, Dalian University of Technology, Dalian 116024, China*
[b] *Department of Mechanical Engineering, University of Dalian, Dalian 116622, China*

Received 20 February 2002; accepted 27 November 2002

Abstract

Electron concentration and atomic size rules are important criteria for bulk metallic glass formation. According to these rules, a series of new Zr-Al-Ni-Cu amorphous alloys with a constant e/a ratio of 1.4 and an average atomic size of 0.1496 nm was designed. All the alloys have high glass forming abilities, large supercooled liquid regions ΔT_x, and large reduced glass transition temperatures T_{rg}. The best glass forming composition is located near $Zr_{63.8}Al_{11.4}Ni_{17.2}Cu_{7.6.}$ Its glass forming ability is higher than that of the Inoue alloy $Zr_{65}Al_{7.5}Ni_{10}Cu_{17.5}$.

Keywords: Bulk metallic glasses; Zr-Al-Ni-Cu alloys; Electron concentration; Atomic size

1. Introduction

Bulk metallic glasses (BMGs) have been found in the Ln-Al-TM, Zr-Al-TM, Ti-Zr-TM systems by Inoue's group [1]. However, their formation mechanism is still not clear and there is no qualitative criterion for judging BMG formation compositions [2]. This hinders the further development of new BMGs.

Negal and Tauc in the 1970s addressed this problem by examining the electronic structure of metallic glasses consisting of noble and polyvalent metals [3]. They showed that metallic glasses are a group of Hume–Rothery phases, like many crystalline intermetallics. The optimum e/a ratio, e/a being the average valence electron number per atom, is about 1.7. Later, Hausler further termed the optimum metallic glasses 'ideal amorphous state' [4]. Van der Kolk et al. attempted to combine the contributions of electronic and size effects as two main parameters in judging glass forming ability [5].

In the investigation of quasicrystals, stable quasicrystals in ternary alloy systems were found to have similar e/a ratios specifically called an e/a-constant line [6]. This has led to the prediction of ternary quasicrystal compositions using the e/a-constant line [7[7]]. The stable quasicrystal compositions are located near the crossing points of this line and another straight line linking a binary quasicrystal composition and the third element, termed specific e/a-variant line. These two criteria can precisely determine the composition of a ternary phase.

In this paper this rule is extended to BMG for-

* Corresponding author. Tel.: +1-86-411-470-8389; fax: +1-86-411-470-8389.
E-mail address: dong@dlut.edu.cn (C. Dong).

1359-6454/03/$30.00
doi:10.1016/S1359-6454(02)00596-7

ming systems. Here two criteria are introduced, a specific e/a-constant and an average atomic size. We will first trace the origins of the two criteria, and then verify them by examining a series of new BMG compositions in the Zr-Al-Ni-Cu system.

2. Formation rule of BMGs in Zr-based alloy systems

Amorphous alloys with high glass forming ability can be regarded as alloy phases with specific compositions. The formation of amorphous phases is sensitively dependent on electronic and atomic structure. Early work by Nagel and Tauc analyzed binary $M_{1-x}X_x$ metallic glasses, M representing transition or noble metals, X elements in groups IV or V [3]. They pointed out that an amorphous state is stabilized by the interaction of the Fermi surface and pseudo Brillouin zone boundaries. The Fermi level corresponds to a low density of states, and the Fermi surface is in contact with the pseudo Brillouin zone. This situation can be expressed by $k_p \approx 2\ k_f$, where k_r is the Fermi radius, k_p the amplitude of the wave vector of the Brillouin zone. These results derived by Nagel and Tauc not only show that metallic glasses are Hume–Rothery phases, but also prove that stable glass compositions correspond to a specific electron concentration e/a. Haussler, after examining a series of noble metals-polyvalent element amorphous systems, determined that at a specific e/a of 1.8, the glass forming ability was the highest and the Fermi surface is in contact with the Pseudo-Brillouin zone defined by the amorphous peak [4]. He termed this state the 'ideal amorphous state'.

Atomic size is also an important factor in determining glass forming compositions. Amand and Giessen, after investigating alkaline earth systems, pointed out that atomic size difference influences liquid viscosity and hence amorphous alloy formation [8]. Ramachandrarao [9] first introduced the Varley's model in metal–metal systems. He stressed the importance of atomic size and compressibility of constituent elements and introduced the concept of change in mean atomic volume. Egami and Waseda [10] summarized the influences of atomic size in many binary amorphous systems. They even obtained a semi empirical equation that described the relationship between minimum solute concentration C_B^{min} for the optimum amorphous composition and atomic size factor λ_0: $C_B^{min} \times |\Delta V_{AB}/V_A| = \lambda_0$, where $\Delta V_{AB}/V_A = (r_B^3 - r_A^3)/r_A^3$, r_A and r_B being the atomic radii of the binary constituent elements. They found that for different binary systems, λ_0 is close to 0.10. Liou and Chien [11] pointed out that the atomic size difference is the most important factor in determining composition ranges for the glassy state in vapor-quenched binary glasses. They take atomic volume as the quantitative evaluation basis and predict quite successfully the experimentally observed glass forming range.

Mizutani et al. have analyzed electronic structure and electron transport properties of glasses formed in Late Transition metals–Early Transition metals systems and Ca-based alloys [12–14]. They believe that both electronic and atomic size factors have important contributions in predicting glass forming ability. They show that in electronically simple alloy systems, the glass forming range corresponds to $2k_f/k_p = 0.8$–1.2 ($2k_f$ and k_p are respectively the Fermi sphere diameter and amorphous peak position), and $2k_f/k_p$ slightly larger than 1 is the most common case. At the same time, they considered an atomic size factor as supplemental to the electronic factor, quantified by the atomic size ratio r/R of small and large atoms, which is in the range of 0.5–0.8. They also employed the empirical equation of Egami and Waseda in $Ag_{50}Cu_{50}$-based ternary Hume–Rothery amorphous alloys and found satisfactory agreement between liquid quenched samples and predicted results.

In the Zr-Al-Ni-Cu alloy system, the BMG with the highest glass forming ability known so far is the Inoue alloy $Zr_{65}Al_{7.5}Ni_{10}Cu_{17.5}$ with a ΔT_x of 127 K [15]. During an investigation of the microstructure of an as-cast $Zr_{65}Al_{7.5}Ni_{10}Cu_{17.5}$ ingot, we found five crystalline phases in coexistence with the glassy phase [16]. What is remarkable about these phases, as we have noted, is that they are all Hume–Rothery phases with c/a ratios (listed in Table 1) close to 1.4, the e/a ratio of the Inoue alloy. This is strikingly similar to the e/a-constant phenomenon in quasicrystalline systems [6]. Based

Table 1
The e/a and R_a values of some typical amorphous alloys and crystalline phases in Zr-Al-Ni, Zr-Al-Cu, and Zr-Al-Ni-Cu. The Goldschmidt atomic radii are 0.16 for Zr, 0.143 for A1, 0.125 for Ni, and 0.128 nm for Cu

Composition	Phase	e/a	Av. atomic size (nm)
$Zr_{60}Al_{20}Ni_{20}$	amorphous	1.50	0.1496
$Zr_{55}Al_{20}Ni_{25}$	amorphous	1.43	0.1479
$Zr_{60}Al15Ni_{25}$	amorphous	1.35	0.1487
$Zr_{65}Al_{7.5}Cu_{27.5}$	amorphous	1.48	0.1499
$Zr_{60}Al_{10}Cu_{30}$	amorphous	1.50	0.1487
$Zr_{73}Al_{13}Cu_{14}$	amorphous	1.63	0.1533
$Zr_{67.0}Al_{1.7}Ni_{8.4}Cu_{22.9}$	Zr_2Cu type	1.28	0.1494
$Zr_{65.4}Al_{11.7}Ni_{11.6}Cu_{11.3}$	Zr_6Al_2Ni type	1.45	0.1503
$Zr_{65}Al_{7.5}Ni_{10}Cu_{17.5}$	amorphous	1.38	0.1496

on this observation we obtain the first criterion for BMG formation: a BMG and its crystalline counterparts have nearly constant c/a ratios specific to a given alloy system. In a binary system, the specific e/a ratio determines the composition of the best glass forming composition. In a ternary system, e/a-constant compositions generate a straight line, or e/a-constant line. In a quaternary system, it is an e/a-constant plane. We notice that the known amorphous phases in the Zr-Al-Ni, Zr-Al-Cu, and Zr-Al-Ni-Cu systems, and the crystalline phases in the Zr-Al-Ni-Cu system all have e/a ratios in the range of 1.3–1.5, close to the value of 1.4 of the Inoue alloy. The e/a values of these phases are listed in Table 1.

We further notice that these amorphous and crystalline phases are not distributed randomly on the c/a-constant plane in the quaternary phase diagram. As shown in Fig. 1, their compositions are located close to a specific straight line on the plane. This special composition distribution reflects the influence from factors other than electron concentration. As mentioned previously, atomic size is an important factor in forming amorphous structures [8–11,17]. By analogy to the calculation of average number of conduction electrons per atom, we introduce the concept of average atomic size as the second criterion for judging glass forming compositions, defined as the sum of the product of atomic fraction C_i and Goldschmidt atomic radius R; for each element $R_a = \Sigma C_i^* R_I$. We then calculated R_a values for the phases mentioned above. The constant atomic size phenomenon is then revealed: all

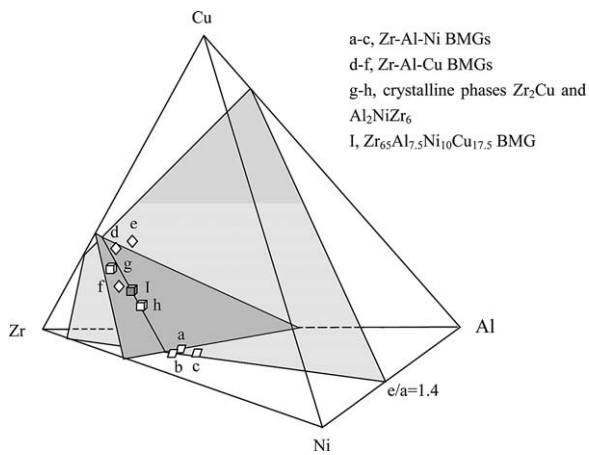

Fig. 1. Zr-Al-Ni-Cu quaternary phase diagram.

the compositions have R_a in the range of 0.1487–0.1533 nm, close to 0.1496 nm, the Ra value for the Inoue alloy. The e/a and R_a values of some typical amorphous alloys and crystalline phases in Zr-Al-Ni, Zr-Al-Cu, and Zr-Al-Ni-Cu are listed in Table 1. The specific composition line is at the crossing of two planes, one being e/a-constant and the other R_a constant.

We take the e/a and R_a values of the Inoue alloy $Zr_{65A}l_{7.5N}i_{10}Cu_{17.5}$ and plotted the two planes in the quaternary phase diagram in Fig. 1. All the compositions of known BMGs and quaternary phases are located near the line where the e/a = 1.4 and $R_a^{=}$ 0.1496 mn planes intersect, corresponding to the values of the Inoue alloy. By doing so we established the two quantitative criteria for the for-

mation of BMGs in Zr-based ally systems based on the Inoue alloy.

We need to know the conduction electron concentration contributions from transition metals Ni, containing 3d electrons, and Zr, containing 4d electrons. After examination of the literature [18] and our theoretical and experimental verification [19], we have determined that e/a values for Zr and Ni are respectively 1.5 and 0. For A1 and Cu, these values are well established, being +3 and +1, respectively.

3. Experiment methods

Six Zr-Al-Ni-Cu compositions were designed which satisfy e/a = 1.4 and R_a = 0.1496 nm. Their compositions are listed in Table 2. Alloy 1 was chosen close to the Zr-Al-Cu end of the line, and alloy 6 close to the Zr-AI-Ni end. Among them, alloy 3 is the Inoue alloy. The change in Zr content is small. From alloy 1 to 6, the A1 and Ni contents increase and the Cu content decreases.

Master alloys were prepared by arc melting of high purity Zr (4N), Al (5N), Ni (4N), and Cu (4N). These alloys were then suction cast into ϕ3 mm bars. The structure was characterized using XRD (Cu Kα radiation with wavelength of 0.15406 nm), optical microscope, and TEM (J1000X). Thermal stability was analyzed with a Perkin-Elmer DSC7-type differential scanning calorimeter (heating rate 0.67 K/s). The melting point and liquid temperature were measured on Netzsch STA409C-type differential thermal analyzer. The heating rate is 0.67 K/s, and the temperature accuracy reaches 0.3% of the measured temperature.

4. Structure analysis

Fig. 2 presents XRD patterns taken on the cross sections of the ingots. In all these patterns, there is one broad peak at $2\theta = 36.7°$, obtained by fitting the peak with Gaussian profile using Microsoft

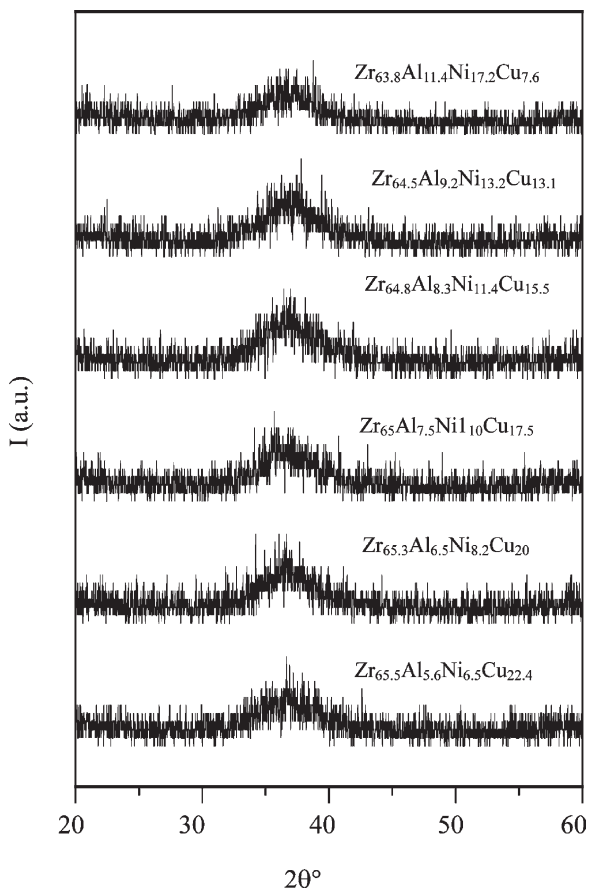

Fig. 2. XRD patterns of the six alloys.

Table 2
Compositions of the six alloys with constant e/a and R_a being close to the values of the Inoue alloy (e/a = 1.4 and R_a = 0.1496 nm). The alloy 3 is the lnoue alloy

Number	1	2	3
Alloys	$Zr_{65.5}Al_{5.6}Ni_{6.5}Cu_{22.4}$	$Zr_{65.3}Al_{6.5}Ni_{8.2}Cu_{20}$	$Zr_{65}Al_{7.5}Ni_{10}Cu_{17.5}$
Number	4	5	6
Alloys	$Zr_{64.8}Al_{8.3}Ni_{11.4}Cu_{15.5}$	$Zr_{64.5}Al_{9.2}Ni_{13.2}Cu_{13.1}$	$Zr_{63.8}Al_{11.4}Ni_{17.2}Cu_{7.6}$

Fig. 3. Cross-section optical image of sample 2.

Excel, and no obvious sharp peaks are present. The optical microscope observations also confirm that the cross-sections were homogeneous, as exemplified by the cross-sectional image of sample 2 shown in Fig. 3. Therefore, all these samples consisted mainly of an amorphous phase.

We further analyzed the structure by TEM. No crystalline phases were observed in samples 3 to 6. Samples 1 and 2 contain crystalline phases only at the top ends (this part of the ingots solidifies last) and are completely amorphous at the bottom ends. Fig. 4 is the selected area electron diffraction

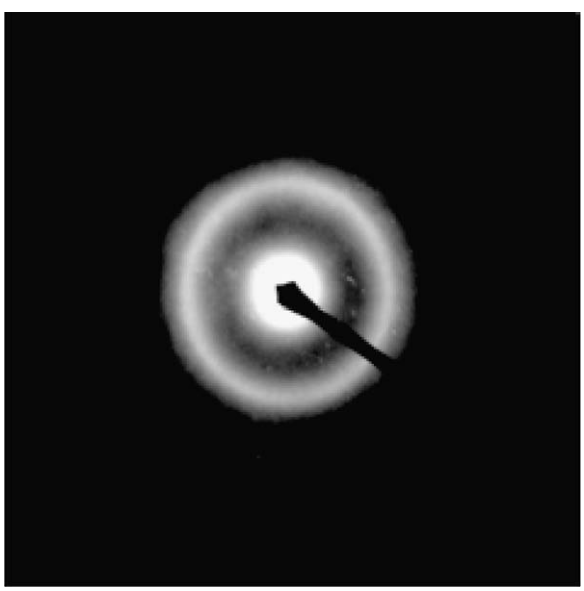

Fig. 4. Typical amorphous ring pattern taken from sample 1.

(SAED) pattern of the amorphous phase and Fig. 5 is the SAED pattern of a crystalline phase in sample 1. The crystalline phase is of Zr_2AI type with space group 14/mcm and ideal lattice parameters 0.685 and 0.550 nm. In sample 2, we see an FCC crystalline phase (Fig. 6). Its lattice parameter a = 0.364 nm is close to that of Cu (0.361 mn) and Ni (0.352 nm).

5. Thermal stability and glass forming ability analysis

The thermal stability and glass forming ability are critical temperatures measured with DSC and DTA. Fig. 7 presents DSC curves of the six samples. Except sample 3, which shows two crystallization peaks,[1] all the other samples manifest only one small and one large peak, i.e. the first phase transition is an endothermal glass transition reaction, followed by α wide supercooled liquid region, and at the T_x temperature, crystallization occurs which is exothermic.

The glass transition temperature T_g, crystallization temperature T_x, and supercooled liquid region ΔT_x of the six samples are listed in Table 3. We see that ΔT_x values are all quite large, close to 100 K, the largest being 105 K for sample 2. This means that we have found a series of e/a-constant and R_a-constant BMGs with large supercooled liquid regions, and the well-known Inoue alloy is only one of them.

In order to assess the relative thermal stability and glass forming ability among the six samples, we compared T_g and T_x derived from the DSC curves. The higher the transition temperatures, the higher the thermal stability of the metallic glass. The stability of the BMGs increases from sample 1 to 6, and the best of them is 6, instead of the Inoue alloy (3).

The glass forming ability is related to the reduced glass transition temperature T_{rg} [20]. The DTA curves are shown in Fig. 8. Melting temperature T_m, liquid temperature T_I, liquid zone $T_l - T_m$,

[1] The origin of the double peaks in the DSC curves of sample 3 is not known. The result is repeatable.

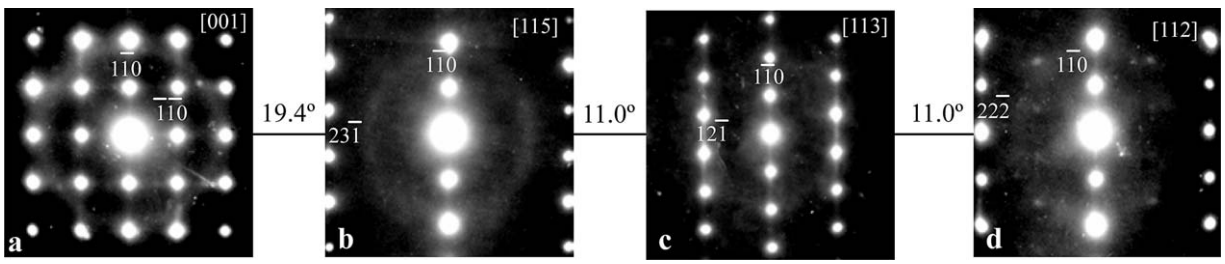

Fig. 5. SAED patterns of the Zr_{2A}l-type phase in sample 1.

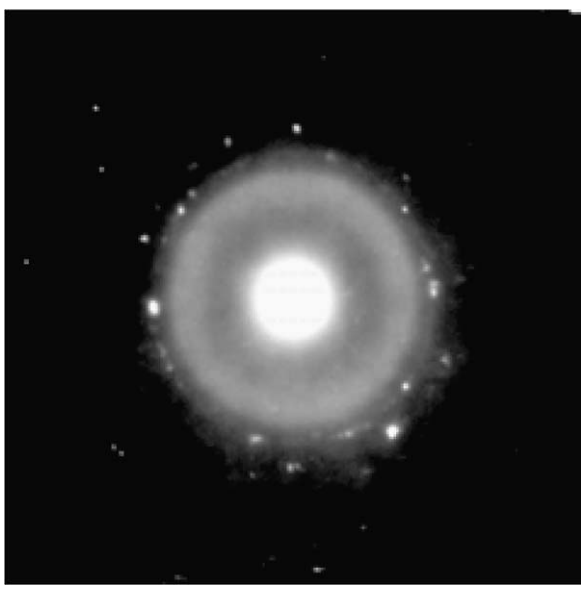

Fig. 6. The FCC phase with Cu structure observed in sample 2.

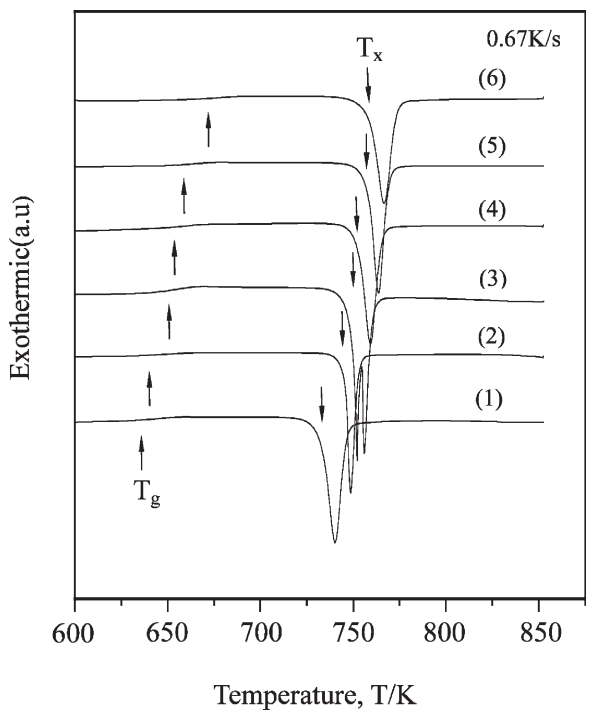

Fig. 7. DSC curves of the six samples. Glass transition temperature T_g, crystallization temperature T_x are marked.

and the reduced glass transition temperature $T_{rg} = T_g/T_m$ or $T_{rg} = T_g/T_l$ are listed in Table 4 and plotted in Figs. 9 and 10. T_g/T_m and T_g/T_l are two forms for expressing the reduced glass transition temperature T_{rg}. According to Lu et al. [21], T_g/T_l is more linked to the glass forming ability than T_g/T_m. In our case both data manifest similar trends. Samples 1 and 2 show multiple melting peaks while 3 to 6 only two. The melting temperature T_m increases from 1 to 6 and the difference between T_l and T_m decreases, indicating that the latter group of samples are closer to the eutectic composition. The smallest $T_l - T_m = 48$ K is found for sample 5 and the highest reduced glass transition temperatures, either T_g/T_m, or T_g/T_l, are found for sample 6. These results indicate that the eutectic composition, or the best glass forming composition, may be located between 5 and 6. This is consistent with the tendency manifested by T_g and T_x. This is also proved by XRD and TEM results showing that samples 1 and 2 contained crystalline phases but the others did not.

We have shown that all six samples are BMGs with large ΔT_x and T_{rg}, and high T_g and T_x. Therefore our criteria for BMG compositions, based respectively on conduction electron concentration

Table 3
T_g, T_x, and ΔT_x of the six samples derived from DSC curves

Number	Alloy	T_g (K)	T_x (K)	ΔT_x (K)
1	$Zr_{65.5}Al_{5.6}Ni_{6.5}Cu_{22.4}$	636	733	97
2	$Zr_{65.3}Al_{6.5}Ni8_{.2}Cu_{20}$	640	745	105
3	$Zr_{65}Al_{7.5}Ni_{10}Cu_{17.5}$	650	750	100
4	$Zr_{64.8}Al_{8.3}Ni_{11.4}Cu_{15.5}$	653	752	99
5	$Zr_{64.5}Al_{9.2}Ni_{13.2}Cu_{13.1}$	658	757	99
6	$Zr_{63.8}Al_{11.4}Ni_{17.2}Cu_{7.6}$	671	758	87

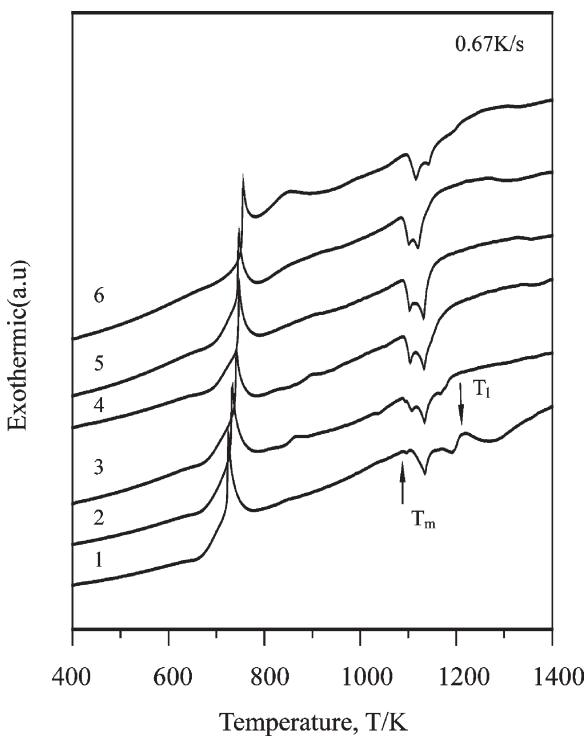

Fig. 8. DTA curves.

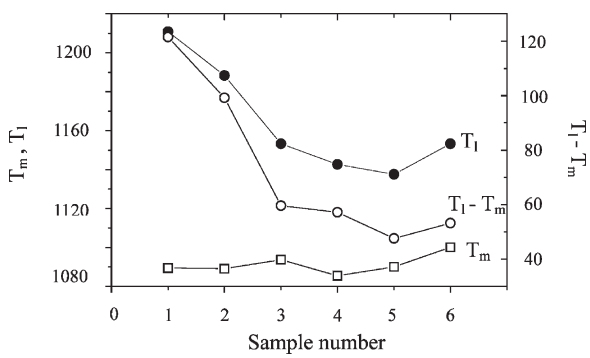

Fig. 9. T_m, T_l, and T_l–T_m of the six samples.

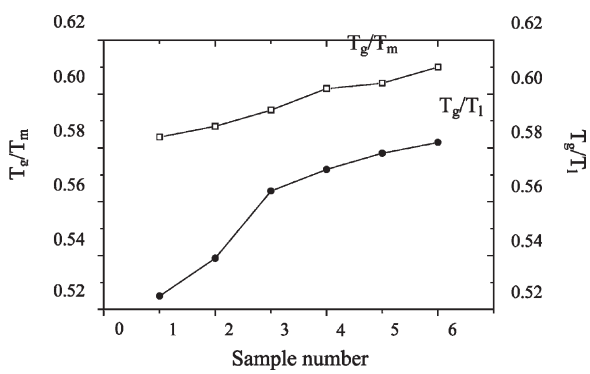

Fig. 10. Reduced glass transition temperatures of the six samples.

and atomic size factors, can correctly and precisely predict the composition of BMGs. Among the six samples, sample 2 has the highest ΔT_x, but it contains a crystalline phase and its reduced glass transition temperature is not the highest. The inconsistency of ΔT_x and T_{rg} has been noted in other alloy systems as well [22,23]. The best BMG composition, based upon T_{rg}, T_x, and T_g, is located between 5 and 6, and closer to 6.

We have tried to produce ϕ6 mm bars using the same suction casting technique, and have successfully obtained BMGs for compositions 5 and 6, but all the other samples manifested partial crystallization. This further proves that T_{rg}, instead of ΔT_x, more sensitively measures the glass forming ability of BMGs.

Table 4
Melting temperature T_m, liquid temperature T_l, liquid zone $T_l - T_m$, and the reduced glass transition temperature $T_{rg} = T_g/T_m$ or $T_{rg} = T_s/T_l$ as measured from DTA curves shown in Fig. 8

Number	Alloy	T_m (K)	T_l (K)	T_g/T_m	T_g/T_l	$T_l - T_m$
1	$Zr_{65.5}Al_{5.6}Ni_{6.5}Cu_{22.4}$	1090	1211	0.584	0.525	122
2	$Zr_{65.3}Al_{6.5}Ni8_{.2}Cu_{20}$	1090	1188	0.588	0.539	99
3	$Zr_{65}Al_{7.5}Ni_{10}Cu_{17.5}$	1094	1153	0.594	0.564	60
4	$Zr_{64.8}Al_{8.3}Ni_{11.4}Cu_{15.5}$	1086	1143	0.602	0.572	57
5	$Zr_{64.5}Al_{9.2}Ni_{13.2}Cu_{13.1}$	1090	1138	0.604	0.578	48
6	$Zr_{63.8}Al_{11.4}Ni_{17.2}Cu_{7.6}$	1100	1153	0.610	0.582	53

6. Nagel-Tauc rule in Zr-Al-Ni-Cu BMGs

As pointed out by Nagel and Tauc, the most stable metallic glass should satisfy $k_p \approx 2\ k_f$, where k_ρ represents the peak position, and $2k_f$ the Fermi sphere diameter. Table 5 shows the measured k_p values from the XRD patterns and calculated $2k_f$ for the six compositions. According to the free electron model, $k_f = (3\pi^2 N)^{1/3}$, where N is the number of electrons per unit volume, equal to e/a times the atomic density (an example of the calculation can be found in Ref. [16]). The peak position $k_p = 4\pi \sin\theta/\lambda$, and the diffraction angle is fitted out from the principal diffuse peak using a Gauss profile [24]. We see good agreements with the Nagel-Tauc rule in these BMGs, indicating that the mechanism behind the e/a criterion is the Nagel-Tauc rule. Further work is being done to understand the implications of the specific average atomic size factor.

7. Conclusions

We have shown by examples of a series of Zr-Al-Ni-Cu alloys with constant conduction electron concentration e/a and constant average atomic size R_a, that e/a and R_a factors serve as the criteria for judging BMG forming compositions. The Nagel-Tauc rule is the mechanism behind the constant e/a criterion. In the Zr-Al-Ni-Cu system, the specific e/a ratio is close to 1.4 and R_a close to 0.1496 nm. All six samples with the e/a and R_a values have large supercooled liquid regions AT (about 100 K) and reduced glass transition temperatures T_{rg} (about 0.6), high glass transition and crystallization temperatures. The best glass forming composition in this system is $Zr_{63.8}Al_{11.4}Ni_{17.2}Cu_{7.6}$, instead of $Zr_{65}Al_{7.5}Ni_{10}Cu_{17.5}$, the Inoue alloy. This new BMG has $T_{rg} = T_g/T_m = 0.61$, $\Delta T_x = 87$ K, $T_g = 671$ K, $T_x = 758$ K.

Table 5
Density ρ, Fermi sphere diameter $2k_f$, and amorphous peak position k_p of the six samples. The density data are obtained using mass density bottle method at room temperature, with accuracy of 0.1 wt.%

Number	Alloy	ρ (g/cm^3)	$2k_f$ (nm^{-1})	k_p (nm^{-1})	$k_p - 2k_f$ (nm^{-1})
1	$Zr_{65.5}Al_{5.6}Ni_{6.5}Cu_{22.4}$	6.850	25.674	25.768	0.094
2	$Zr_{65.3}Al_{6.5}Ni8_{.2}Cu_{20}$	6.876	25.757	25.686	−0.071
3	$Zr_{65}Al_{7.5}Ni_{10}Cu_{17.5}$	6.744	25.649	25.697	0.048
4	$Zr_{64.8}Al_{8.3}Ni_{11.4}Cu_{15.5}$	6.823	25.795	25.755	−0.040
5	$Zr_{64.5}Al_{9.2}Ni_{13.2}Cu_{13.1}$	6.754	25.763	25.862	0.099
6	$Zr_{63.8}Al_{11.4}Ni_{17.2}Cu_{7.6}$	6.677	25.797	25.710	−0.087

Acknowledgements

The present work is supported by Natural Science Foundation of China under grant number 50271012.

References

[1] Inoue A, Zhang T. Stabilization of supercooled liquid and bulk glassy alloys in ferrous and non-ferrous systems. Journal of Non-Crystalline Solids 1999;250-252:552–9.
[2] Inoue A, Shibata T, Zhang T. Effect of additional elements on glass transition behavior and glass formation tendency of Zr-Al-Cu-Ni alloys. Materials Transactions JIM 1995;36:1420–6.
[3] Nagel SR, Taue J. Nearly-free-electron approach to the theory of metallic glass alloys. Phys Rev Lett 1975;35:380–3.
[4] Haussler P. On evidence for a new Hume-Rothery phase with an amorphous structure. Z. Phys. B 1983;53:15.
[5] Van der Kolk GJ, Miedema AR, Niessen A. On the composition range of amorphous binary transition alloys. J. Less-Common Metals 1988;145:1–17.
[6] Dong C. The concept of the approximants of quasicrystals. Scripta Metall.& Mater 1995;33:239.
[7] Qiang JB, Wang DH, Bao CM, Wang YM, Xv WP, Song ML, Dong C. Formation rule for Al-based ternary quasicrystals: example of Al-Ni-Fe decagonal phase. J. Mater. Res 2001;16:2653–60.
[8] Amand St R, Giessen BC. Easy Glass Formation in Simple Metal Alloys: Amorphous metals containing Calcium and Strontium. Scripta Met 1978;12(1021):1021.
[9] Ramachandrarao P. On glass formation in metal-metal systems. Z Metallked 1980;71:172–7.
[10] Egami T, Waseda Y. Atomic size effect on the formability of metallic glasses. J Non-Cryst Solid 1984;64:113–4.
[11] Liou SH, Chien CL. Composition range of binary amorphous alloys. Phy Rev B 1988;35:2443–6.
[12] Yamada Y, Itoh Y, Mizutani U. Electronic structure of (Ni33Zr67)1-X, (X=Ti, V, Cr, Mn, Fe, Co, Ni or Cu) ternary metallic glasses studied by low temperature specific heat measurement. Mater Sci and Eng 1988;99:289–93.
[13] Mizutani U, Sasaura M. Electronic structure and electron transport in Ca-Mg-Cu metallic glasses. Mater Sci and Eng 1988;99:295–9.
[14] Mizutani U, Sugiura H, Yamada Y. Electronic structure and electron transport properties of Al-Cu-Y and Mg-Cu-Y amorphous alloys. Mater Sci and Eng 1994;79:132–6.
[15] Zhang T, Inoue A, Masumoto T. Amorphous Zr-Al-TM (TM=Co,Ni,Cu) alloys with significant supercooled liquid region of over 100 K. Mater Trans JIM 1991;32:1005–10.
[16] Shek CH, Wang YM, Dong C. The e/a-constant Hume-Rothery phases in an As-cast Zr65AIT5NiIOCu17.5 alloy. Mater Sci and Eng 2000;A291:78–85.
[17] Inoue A, Zhang T, Masumoto T. Zr-Al-Ni amorphous alloys with high glass transition temperature and significant supercooled liquid region. Mater Trans JIM 1990;31:177–83.
[18] Pettifor DG. Theory of energy bands and related properties ofd transition metals: I. Band parameters and their volume dependence. .J. Phys. F: Metal Phys 1977;7:613–33.
[19] Wang YM, Qiang JB, Xu WP, Dong C, Wong CH, Shek CH. Composition rule of bulk metallic glasses and quasicrystals using electron concentration criterion. J Mater Res 2003, in press.
[20] Turnbull D. Solidification. Metals Park, OH: American Society for Metals, 1971.
[21] Lu Z P, Tan H, Li Y, Ng SC. The correlation between reduced glass transition temperature and glass forming ability of bulk metallic glasses. Scripta Mater 2000;42:667–73.
[22] Inoue A, Zhang T, Kim YH. Synthesis of high strength bulk amorphous Zr-Al-Ni-Cu-Ag alloys with a nanoscale secondary phase. Mater Trans JIM 1997;38:749–55.
[23] Zhang T, Inoue A. Mechanical properties of Zr-Ti-Al-Ni-Cu bulk amorphous sheets prepared by squeeze casting. Mater Trans JIM 1998;39:1230–7.
[24] Buschow KHJ. Effect of short-range ordering on the thermal stability of amorphous Ti-Cu alloys. Scr. Met 1933;17:1135.